*lil*Gym: Natural Language Visual Reasoning with Reinforcement Learning

Anne Wu, Kianté Brantley, Noriyuki Kojima, and Yoav Artzi
Department of Computer Science and Cornell Tech, Cornell University
{aw588, kdb82, nk654}@cornell.edu, {yoav}@cs.cornell.edu

1 Introduction

Reinforcement learning (RL) with natural language context poses important opportunities and challenges. Language provides an expressive and accessible conduit for task specification, so that RL agents can address a broad set of tasks, rather than learn a single behavior. For natural language processing (NLP), RL is a promising avenue for language use and acquisition with world interaction. Fulfilling this potential requires addressing core reasoning challenges: the RL agent must reason about both high-level language concepts, low-level actions, and the relations between them.

Despite significant interest and promising approaches, it has been challenging to create expressive RL benchmarks with natural language. Existing approaches often make various simplifications, such as using synthetic language [Côté et al., 2018, Co-Reyes et al., 2019] or heuristic approximation, for example via demonstration data [Misra et al., 2017]. While these approaches open new avenues for research, they either do not explore the full complexity of natural language or introduce unexpected artifacts into learning through meaning approximations.

We present *lil*Gym,[1] a reinforcement learning benchmark for natural language visual reasoning that addresses the above issues. It includes the semantically diverse natural language of the Natural Language for Visual Reasoning (NLVR) corpus [Suhr et al., 2017], which has highly compositional human-written language and requires complex grounded reasoning. *lil*Gym provides an executable evaluation function for every statement in the NLVR corpus, and these annotations align the reward function with the language semantics of the agent's underlying reasoning task. We experiment with standard on-policy RL algorithms. Our experimental results show that while existing methods are able to achieve non-trivial performance, the complex visual reasoning required by *lil*Gym forms a challenging open problem.

2 The *lil*Gym Benchmark

*lil*Gym consists of a collection of environments that share a common backbone. The backbone is a 2D plane that is manipulated by placing and removing objects of different types. Each environment instance is a Markov Decision Process (MDP) created by pairing a natural language statement and a target boolean value with a configuration of the shared backbone. The goal of the agent in each environment is to manipulate it by adding and removing objects so that the truth-value of the statement with regard to the environment is the target boolean.

The learning problem *lil*Gym presents is to induce a policy that generalizes across MDPs. We split the MDPs to training, development, and held-out testing sets. The training environments are to be used for parameter estimation, while the two other sets are for testing during development and for final held-out testing to report approach performance.[2]

[1] *lil*Gym stands for Language, Interaction, and Learning Gym.
[2] We recommend reporting both development and held-out test results in future work for easy comparison.

36th Conference on Neural Information Processing Systems (NeurIPS 2022).

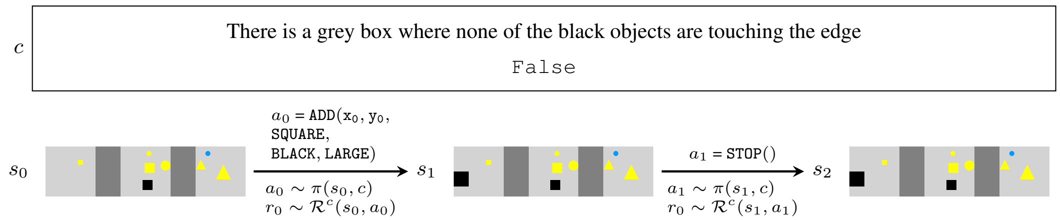

Figure 1: Overview of an example for one CMDP, `SCATTER-FLIPIT`. The context c consists of a text statement and a target boolean. The leftmost image depicts the initial state s_0. The agent π is presented with (s_0, c), and chooses an action $a_0 \sim \pi(\cdot|s_0, c)$. The environment transitions to the next updated state s_1, the context remaining the same.

There are two dimensions of configuration: appearance and starting condition. The appearance determines the state space, transition function, and action space. The appearance of the environment can be (a) `TOWER`: the objects include squares only, and they can be stacked into towers in specific positions only; or `SCATTER`: objects of different types can be freely distributed. The starting condition determines the agent's goal. The starting condition and agent objective can be: (a) `SCRATCH`: the environment starts without any objects and the goal is to modify it so that the statement's truth-value is `True`; or (b) `FLIPIT`: the environment starts with a set of objects and the agent's goal is to flip the truth-value of the statement.

There are four configurations: `TOWER-SCRATCH`, `TOWER-FLIPIT`, `SCATTER-SCRATCH`, and `SCATTER-FLIPIT`. Each configuration forms a Contextual Markov Decision Process [CMDP; Hallak et al., 2015]. CMDP is an abstraction over a set of MDPs to account for a context that remains constant throughout the interaction with an MDP. We set the context to include the statement and the target boolean the interaction is conditioned on. A CMDP is a tuple $(\mathcal{C}, \mathcal{S}, \mathcal{A}, \mathcal{M}(c))$, where $\mathcal{C}$ is the context space, $\mathcal{S}$ the state space, $\mathcal{A}$ the action space, and $\mathcal{M}$ a function mapping a context $c \in \mathcal{C}$ to an MDP $\mathcal{M}(c) = (\mathcal{S}, \mathcal{A}, T, R^c, \beta^c)$. Here, $T : \mathcal{S} \times \mathcal{A} \rightarrow \mathcal{S}$ is a transition function, $R^c : \mathcal{S} \times \mathcal{A} \rightarrow \mathbb{R}$ the reward function, and β^c an initial state distribution. This means that a CMDP is a set of MDPs that share the same states and actions. Table 2 in Appendix A shows the number of MDPs under each configuration. The policy takes as input both the current state and the context that created the MDP. The learning problem is to estimate parameters θ for a policy $\pi_\theta : \mathcal{S} \times \mathcal{C} \rightarrow \mathcal{A}$.

Contexts A context $c \in \mathcal{C}$ is a pair $c = (\bar{x}, b)$, where $\bar{x}$ is a natural language statement and $b \in \{\texttt{True}, \texttt{False}\}$ is a target boolean value for the statement $\bar{x}$ with respect to the state s. The target boolean value in `SCRATCH` is always `True`. In `FLIPIT`, the target boolean value can either be `True` or `False`.

States A state $s \in \mathcal{S}$ is an RGB image. Images in *lil*Gym are divided into three box regions of identical dimensions by two gray separators (Figure 1). The objects in *lil*Gym have three properties, each can take multiple values: shape (`CIRCLE`, `SQUARE` or `TRIANGLE`), color (`BLACK`, `BLUE`, or `YELLOW`), and size (`SMALL`, `MEDIUM` or `LARGE`). In `TOWER`, states are constrained to have stacks of up to four `SQUARE`s of `MEDIUM` size and any color at the center of each box. `SCATTER` states support all object shapes, sizes, and colors, and they may be positioned freely. In both conditions, objects cannot cross image boundaries or into the separators. The choice between `SCRATCH` or `FLIPIT` does not influence the state space.

Actions and Transitions There are three action types `STOP`, `ADD`, and `REMOVE`. `STOP` terminates the episode and does not require any parameters. The truth-value of the statement is only evaluated and compared to the target boolean after the `STOP` action is taken. `ADD` adds objects to the environment, and `REMOVE` removes objects. They take different arguments for `TOWER` and `SCATTER`:

`TOWER`: Similar to the state space of `TOWER`, the actions are also more constrained. Both `ADD` and `REMOVE` take a position argument, which has three possible values corresponding to the three box regions. Objects are always added or removed at the top of the stack. Adding an object on top of a stack of four objects or removing an object from an empty box are both invalid actions. `ADD` also takes a color argument. Including `STOP`, there are $1 + (3 + 1) \times 3 = 13$ actions.

SCATTER: Unlike TOWER, objects of any type can be placed freely in the box regions. Both ADD and REMOVE take 2D coordinates that specify the pixel location. Adding an object places it so that its top-left coordinates are the given coordinates. Removing an object will remove the object at the given coordinates. Adding also requires specifying the shape, color, and size. If adding results in objects overlap or boundary crossing with the separators or image boundaries, the action is invalid. Removing from a position that does not include an object is also an invalid action. The native resolution of images is 380×100 pixels. Including STOP, there are $1+(380\times 100)\times((3\times 3\times 3)+1) = 1{,}064{,}001$ actions. In our experiments (Section 4), we use a grid of 19×5, giving a total number of 2,661 actions.

The environment transitions are controlled by the transition function $T : \mathcal{S} \times \mathcal{A} \rightarrow \mathcal{S}$. T depends on the choice between TOWER and SCATTER, because this choice determines the action space. The transition function does not modify the context, which is fixed for a given MDP.

Reward Function The reward function R^c is computed with respect to the context pair $c = (\bar{x}, b)$, and is based on evaluating the truth-value of the natural language statement $\bar{x}$ with respect to a state s, and comparing it to the target boolean b. *lil*Gym includes an executable evaluation function $\mathcal{E}^{\bar{x}} : \mathcal{S} \times \mathcal{A} \rightarrow \{\texttt{True}, \texttt{False}\}$ for every statement $\bar{x}$. We describe how we create these evaluation functions in Section A.3.

The agent receives a positive reward for terminating the episode using the STOP action with the statement evaluation $\mathcal{E}^{\bar{x}}(s)$ equal to the target boolean value b. If the statement boolean value $\mathcal{E}^{\bar{x}}(s)$ does not equal the target boolean b value when taking the STOP action, the agent receives a negative reward. If the episode terminates because the current time step t reached the action horizon H or because of an invalid action, the agent also receives a negative reward. Action validity depends on the current state s and on the configuration, because TOWER and SCATTER have different action spaces. There is also a verbosity penalty of δ for every other action. Formally, the reward is:

$$R^c(s,a) = \begin{cases} 1.0 & a = \texttt{STOP} \wedge \mathcal{E}^{\bar{x}}(s) = b \\ -1.0 & a = \texttt{STOP} \wedge \mathcal{E}^{\bar{x}}(s) \neq b \\ -1.0 & (a \text{ is invalid in } s) \vee (t = H) \\ -\delta & \text{otherwise} \end{cases} .$$

Initial State Distribution The initial state distribution β^c is parameterized by the context $c \in \mathcal{C}$, which is different between SCRATCH and FLIPIT. In SCRATCH, the agent modifies an empty environment to satisfy the truth-condition of the statement $\bar{x}$ in the context c, so the initial state s_0 is always an empty image. The set of initial states β^c for every context $c \in \mathcal{C}$ is the set of images associated with the statement $\bar{x}$ in the NLVR data. In practice, for FLIPIT, this set includes between 1 to 43 images.

3 Experimental Setup

We consider two RL algorithms paired with two models for a total of four algorithm-model pairs.

3.1 Models

In our experiments, we consider two models: C+BERT and ViLT. These two models learn a joint visuo-linguistic representation, which is necessary to solve the proposed CMDP configurations.

C+BERT We process the statement $\bar{x}$ using BERT [Devlin et al., 2019], and do mean pooling across all layers and tokens to get the statement representation. We use a three-layer CNN [Fukushima and Miyake, 1982] to embed the image of the current state s. We concatenate the statement representation, image representation, and an embedding for the target boolean b, and process the vector through a multi-layer perceptron (MLP) to compute the action distribution.

ViLT ViLT is a pretrained multi-modal Transformer that jointly processes text and image inputs [Kim et al., 2021]. We create a sequence of tokens by concatenating the statement, a token for the target boolean, and image patches, separated by special tokens. The image patches are the same size as the 19×5 grid cells, including in TOWER, where the action space does not use a grid.

Table 1: Accuracies for all the four CMDP, with both models (C+BERT and ViLT) and both algorithms (PPO and PPO+SF). Evaluation is done without stop forcing (i.e. with PPO).

		TOWER-SCRATCH		TOWER-FLIPIT		SCATTER-SCRATCH		SCATTER-FLIPIT	
		Dev	Test	Dev	Test	Dev	Test	Dev	Test
PPO	C+BERT	71.78	63.27	35.95	34.78	**39.08**	**48.39**	0.00	0.00
	ViLT	**81.60**	**76.54**	**67.60**	**65.80**	35.63	41.29	**3.51**	**6.09**
PPO+SF	C+BERT	80.98	78.70	27.22	26.75	**70.12**	**74.84**	8.31	8.46
	ViLT	**84.05**	**82.41**	**65.09**	**62.91**	64.37	70.97	**27.48**	**29.95**

3.2 Algorithms

We use PPO [Schulman et al., 2017] for parameter estimation,[3] with a separate network as a critic. The critic network is identical to the policy, except that we add a `tanh` activation for the value output. Because of the large action space, especially for `SCATTER`, the agent rarely observes positive reward, which requires taking a `STOP` action at an appropriate state. We design a simple variant of PPO called PPO+SF (PPO with stop forcing) to study this issue. PPO+SF is identical to PPO, except that during training, we mask all actions except `STOP` when the agent reaches a state where selecting `STOP` will give a positive reward. This modification is present only during training. All testing is done under the same conditions, without stop forcing.

4 Experiments

For the experiments we focus on two questions.

How do the algorithm-model pairs perform? For every CMDP, we report accuracy on the development and test sets for both PPO and PPO+SF and both C+BERT and ViLT. For every configuration, we randomly sample 10% of the training data as a held-out validation set kept unchanged throughout the experiments. We stop training using this validation set with early stopping and select the model with the best validation accuracy.

In Table 1, we observe that the additional guidance of PPO+SF compared to PPO helps with exploration, especially on `SCATTER` CMDPs. On `SCATTER-FLIPIT`, PPO+SF improves performance by 23.86% compared to PPO. This illustrates the hard exploration problem that `SCATTER` CMDPs pose. ViLT generally outperforms C+BERT, except on `SCATTER-SCRATCH`. This is relatively expected given the joint reasoning architecture and multi-modal pre-training of ViLT.

What types of mistakes do PPO models make? We sample 50 erroneous development examples from configurations in the `SCATTER-FLIPIT` and `SCATTER-SCRATCH` CMDPs, and analyze their mistakes. In `SCATTER-SCRATCH` trained with PPO, we found that for C+BERT, 76% of the mistakes are due to invalid actions, and 24% due to early termination. Among the invalid actions, 58% are due to trying to put an item that cannot fit in the box, 24% are due to trying to perform an action on a separator, and 18% due to trying to remove an object from a position that does not include an object. For other configurations, the error causes are similar.

5 Conclusion

We introduce *lil*Gym, a reinforcement learning benchmark focused on natural language visual reasoning. *lil*Gym is designed to be accessible for RL researchers, while still displaying the reasoning richness of natural language. Our data annotation approach allows including expressive and diverse natural language, while still providing accurate and automatic reward computation. Our strong baselines show that existing methods can achieve non-trivial performance on *lil*Gym, but there remain significant challenges to be solved and progress to be made.

[3] We use the PPO implementation of Kostrikov [2018].

References

Peter Anderson, Qi Wu, Damien Teney, Jake Bruce, Mark Johnson, Niko Sünderhauf, Ian Reid, Stephen Gould, and Anton van den Hengel. Vision-and-language navigation: Interpreting visually-grounded navigation instructions in real environments. In *The IEEE Conference on Computer Vision and Pattern Recognition*, pages 3674–3683, 2018.

Stanislaw Antol, Aishwarya Agrawal, Jiasen Lu, Margaret Mitchell, Dhruv Batra, C. Lawrence Zitnick, and Devi Parikh. VQA: Visual question answering. In *IEEE International Conference on Computer Vision*, pages 2425–2433, 2015.

Howard Chen, Alane Suhr, Dipendra Misra, Noah Snavely, and Yoav Artzi. Touchdown: Natural language navigation and spatial reasoning in visual street environments. In *Proceedings of the IEEE/CVF Conference on Computer Vision and Pattern Recognition*, pages 12538–12547, 2019.

Maxime Chevalier-Boisvert, Dzmitry Bahdanau, Salem Lahlou, Lucas Willems, Chitwan Saharia, Thien Huu Nguyen, and Yoshua Bengio. Babyai: A platform to study the sample efficiency of grounded language learning. In *7th International Conference on Learning Representations, ICLR*, 2019.

John D. Co-Reyes, Abhishek Gupta, Suvansh Sanjeev, Nick Altieri, John DeNero, P. Abbeel, and Sergey Levine. Guiding policies with language via meta-learning. In *7th International Conference on Learning Representations, ICLR*, 2019.

Marc-Alexandre Côté, Ákos Kádár, Xingdi Yuan, Ben A. Kybartas, Tavian Barnes, Emery Fine, James Moore, Matthew J. Hausknecht, Layla El Asri, Mahmoud Adada, Wendy Tay, and Adam Trischler. Textworld: A learning environment for text-based games. In *CGW@IJCAI*, 2018.

Pradeep Dasigi, Matt Gardner, Shikhar Murty, Luke Zettlemoyer, and Eduard Hovy. Iterative search for weakly supervised semantic parsing. In *Proceedings of the 2019 Conference of the North American Chapter of the Association for Computational Linguistics: Human Language Technologies, Volume 1 (Long and Short Papers)*, pages 2669–2680.

Jacob Devlin, Ming-Wei Chang, Kenton Lee, and Kristina Toutanova. BERT: Pre-training of deep bidirectional transformers for language understanding. In *Proceedings of the 2019 Conference of the North American Chapter of the Association for Computational Linguistics: Human Language Technologies, Volume 1 (Long and Short Papers)*, pages 4171–4186, 2019.

Kunihiko Fukushima and Sei Miyake. Neocognitron: A self-organizing neural network model for a mechanism of visual pattern recognition. In *Competition and cooperation in neural nets*, pages 267–285. Springer, 1982.

Omer Goldman, Veronica Latcinnik, Ehud Nave, Amir Globerson, and Jonathan Berant. Weakly supervised semantic parsing with abstract examples. In *Proceedings of the 56th Annual Meeting of the Association for Computational Linguistics (Volume 1: Long Papers)*, pages 1809–1819, 2018.

Nitish Gupta, Sameer Singh, and Matt Gardner. Enforcing consistency in weakly supervised semantic parsing. In *Proceedings of the 59th Annual Meeting of the Association for Computational Linguistics and the 11th International Joint Conference on Natural Language Processing (Volume 2: Short Papers)*, pages 168–174, 2021.

Assaf Hallak, Dotan Di Castro, and Shie Mannor. Contextual markov decision processes. *arXiv preprint arXiv:1502.02259*, 2015.

Austin W Hanjie, Victor Y Zhong, and Karthik Narasimhan. Grounding language to entities and dynamics for generalization in reinforcement learning. In *International Conference on Machine Learning*, pages 4051–4062. PMLR, 2021.

Drew A. Hudson and Christopher D. Manning. Compositional attention networks for machine reasoning. In *6th International Conference on Learning Representations, ICLR*, 2018.

Vihan Jain, Gabriel Magalhaes, Alexander Ku, Ashish Vaswani, Eugene Ie, and Jason Baldridge. Stay on the path: Instruction fidelity in vision-and-language navigation. In *Proceedings of the Annual Meeting of the Association for Computational Linguistics*, pages 1862–1872, July 2019.

Minqi Jiang, Jelena Luketina, Nantas Nardelli, Pasquale Minervini, Philip HS Torr, Shimon Whiteson, and Tim Rocktäschel. Wordcraft: An environment for benchmarking commonsense agents. *arXiv preprint arXiv:2007.09185*, 2020.

Justin Johnson, Bharath Hariharan, Laurens Van Der Maaten, Li Fei-Fei, C Lawrence Zitnick, and Ross Girshick. Clevr: A diagnostic dataset for compositional language and elementary visual reasoning. In *Proceedings of the IEEE conference on computer vision and pattern recognition*, pages 2901–2910, 2017a.

Justin Johnson, Bharath Hariharan, Laurens van der Maaten, Judy Hoffman, Li Fei-Fei, C. Lawrence Zitnick, and Ross B. Girshick. Inferring and executing programs for visual reasoning. *2017 IEEE International Conference on Computer Vision (ICCV)*, pages 3008–3017, 2017b.

Wonjae Kim, Bokyung Son, and Ildoo Kim. Vilt: Vision-and-language transformer without convolution or region supervision. In *Proceedings of the 38th International Conference on Machine Learning*, pages 5583–5594, 2021.

Ilya Kostrikov. Pytorch implementations of reinforcement learning algorithms, 2018.

Alexander Ku, Peter Anderson, Roma Patel, Eugene Ie, and Jason Baldridge. Room-across-room: Multilingual vision-and-language navigation with dense spatiotemporal grounding. In *Proceedings of the 2020 Conference on Empirical Methods in Natural Language Processing (EMNLP)*, pages 4392–4412, 2020.

Dipendra Kumar Misra, John Langford, and Yoav Artzi. Mapping instructions and visual observations to actions with reinforcement learning. In *Proceedings of the 2017 Conference on Empirical Methods in Natural Language Processing, EMNLP7*, pages 1004–1015, 2017.

Karthik Narasimhan, Tejas D. Kulkarni, and Regina Barzilay. Language understanding for text-based games using deep reinforcement learning. In *Proceedings of the 2015 Conference on Empirical Methods in Natural Language Processing, EMNLP*, pages 1–11, 2015.

Juan Pavez, Héctor Allende, and Héctor Allende-Cid. Working memory networks: Augmenting memory networks with a relational reasoning module. In *Proceedings of the 56th Annual Meeting of the Association for Computational Linguistics (Volume 1: Long Papers)*, pages 1000–1009, 2018.

Ethan Perez, Florian Strub, Harm De Vries, Vincent Dumoulin, and Aaron Courville. Film: Visual reasoning with a general conditioning layer. In *Proceedings of the AAAI Conference on Artificial Intelligence*, volume 32, 2018.

John Schulman, Filip Wolski, Prafulla Dhariwal, Alec Radford, and Oleg Klimov. Proximal policy optimization algorithms. *arXiv preprint arXiv:1707.06347*, 2017.

Mohit Shridhar, Jesse Thomason, Daniel Gordon, Yonatan Bisk, Winson Han, Roozbeh Mottaghi, Luke Zettlemoyer, and Dieter Fox. ALFRED: A benchmark for interpreting grounded instructions for everyday tasks. In *2020 IEEE/CVF Conference on Computer Vision and Pattern Recognition, CVPR*, 2020.

Mohit Shridhar, Xingdi Yuan, Marc-Alexandre Côté, Yonatan Bisk, Adam Trischler, and Matthew J. Hausknecht. Alfworld: Aligning text and embodied environments for interactive learning. In *9th International Conference on Learning Representations, ICLR*, 2021.

Alane Suhr, Mike Lewis, James Yeh, and Yoav Artzi. A corpus of natural language for visual reasoning. In *Proceedings of the 55th Annual Meeting of the Association for Computational Linguistics (Volume 2: Short Papers)*, pages 217–223, 2017.

Alane Suhr, Srinivasan Iyer, and Yoav Artzi. Learning to map context-dependent sentences to executable formal queries. In *Proceedings of the Conference of the North American Chapter of the Association for Computational Linguistics: Human Language Technologies*, pages 2238–2249, 2018.

Alane Suhr, Stephanie Zhou, Ally Zhang, Iris Zhang, Huajun Bai, and Yoav Artzi. A corpus for reasoning about natural language grounded in photographs. In *Proceedings of the 57th Annual Meeting of the Association for Computational Linguistics*, pages 6418–6428, 2019.

Hao Tan and Mohit Bansal. Object ordering with bidirectional matchings for visual reasoning. In *Proceedings of the 2018 Conference of the North American Chapter of the Association for Computational Linguistics: Human Language Technologies, Volume 2 (Short Papers)*, pages 444–451, 2018.

Yiqun Yao, Jiaming Xu, Feng Wang, and Bo Xu. Cascaded mutual modulation for visual reasoning. In *Proceedings of the 2018 Conference on Empirical Methods in Natural Language Processing*, pages 975–980, 2018.

J.M. Zelle and Raymond J. Mooney. Learning to parse database queries using inductive logic programming. In *Proceedings of the National Conference on Artificial Intelligence*, 1996.

Luke S. Zettlemoyer and Michael Collins. Learning to map sentences to logical form: Structured classification with probabilistic categorial grammars. In *Proceedings of the Conference on Uncertainty in Artificial Intelligence*, 2005.

Wenbo Zheng, Lan Yan, Chao Gou, and Fei-Yue Wang. Webly supervised knowledge embedding model for visual reasoning. *2020 IEEE/CVF Conference on Computer Vision and Pattern Recognition (CVPR)*, pages 12442–12451, 2020.

Table 2: Data statistics per CMDP configuration and data split. The number of MDPs corresponds to the number of contexts under each CMDP. For FLIPIT, "Init." corresponds to the total number of initial states across all MDPs for this CMDP.[4]

	TOWER-SCRATCH	TOWER-FLIPIT		SCATTER-SCRATCH	SCATTER-FLIPIT	
	MDPs	MDPs	Init.	MDPs	MDPs	Init.
Train	989	1,910	5,704	1,241	2,340	6,696
Dev	163	317	676	87	164	313
Test	324	619	1,383	155	285	591
Total	1,476	2,846	7,763	1,483	2,789	7,600

A The *lil*Gym Data

The data used for *lil*Gym is based on the Natural Language for Visual Reasoning (NLVR) corpus [Suhr et al., 2017]. The NLVR data was initially collected as a supervised learning benchmark. We formalize an interactive task on top of the NLVR data and collect additional annotations for reward computation.

A.1 Background: the NLVR Corpus

NLVR includes human-written natural language statements paired with synthetic images. Each pair is annotated with the boolean truth-value of the statement with regard to the image (i.e., True if the statement is true with regard to the image, or False otherwise). The images are designed to support complex reasoning, including about spatial and set relations. The original learning task posed by NLVR is to classify statement-image pairs as True to indicate the statement is true with regard to the image, or False otherwise. Various approaches were developed to address the NLVR challenge [Suhr et al., 2017, Tan and Bansal, 2018, Goldman et al., 2018, Pavez et al., 2018, Yao et al., 2018, Hudson and Manning, 2018, Perez et al., 2018, Dasigi et al., Zheng et al., 2020, Gupta et al., 2021], and a separate version using photos was also released [Suhr et al., 2019].[5] NLVR is roughly balanced, and the current state-of-the-art using the raw images is 80.6% accuracy [Zheng et al., 2020], leaving significant room for improvement and illustrating the reasoning challenges the NLVR data presents.

Qualitative analysis of the data [Table 2 in Suhr et al., 2017] shows a more diverse representation of semantic and compositional phenomena compared to related corpora [Antol et al., 2015], including requiring joint visual-linguistic reasoning about spatial relations, quantities, and sets of objects. NLVR also provides an underlying structured representation for every image, which supports easy image manipulation. The combination of a simple interface for image manipulation with complex reasoning via natural language makes NLVR ideal to support an interactive benchmark environment.

A.2 Constructing *lil*Gym from NLVR

We use the NLVR data to create each of the CMDPs (Table 2). SCRATCH CMDPs include contexts for all natural language statements from NLVR, each paired with the empty initial state containing no shapes. FLIPIT CMDPs include the natural language statements with their corresponding images, both from NLVR (an example from SCATTER-FLIPIT in Figure 1). The images are used as initial states. The target boolean is set so that the initial state does not fulfil it.

The split between TOWER and SCATTER also follows from NLVR. Statements corresponding to TOWER images in NLVR are included in our TOWER CMDPs, and the same for SCATTER sentences.

[4] NLVR includes a total of 18,322 images. This allows further expanding the number of initial states to 92,179 initial states through box element permutations. We do not manipulate this property in this work, but future work could take advantage of it. Our reward computation is invariant to such permutations.

[5] We do not use the photographic NLVR2 in this work.

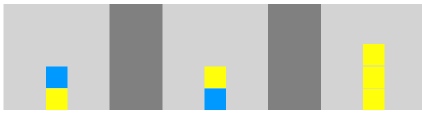

There are two towers with the same height but their base is not the same in color.

```
exist(filter_obj(
    all_boxes, lambda x: x.is_tower() and
    exist(filter_obj(
        all_boxes, lambda y:
            y.is_tower() and
            count(x.all_items_in_box()) ==
                count(y.all_items_in_box()) and
            get_set_colors(filter_obj(
                y.all_items_in_box(),
                is_bottom)) !=
            get_set_colors(filter_obj(
                x.all_items_in_box(),
                is_bottom)))))
```

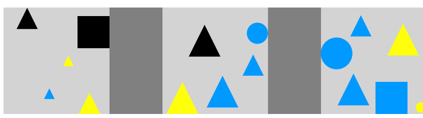

There is a box with all 3 different colors and a black triangle touching the wall with its top.

```
exist(filter_obj(
    all_boxes, lambda x:
        count(get_set_colors(
            x.all_items_in_box())) == 3 and
        exist(filter_obj(
            x.all_items_in_box(), lambda y:
                is_black(y) and
                is_triangle(y) and
                is_touching_wall(y, Side.TOP)))))
```

Figure 2: Example sentences with the example images displayed alongside them during annotation (left), and their annotated Python program representation (right). Both sentences and logical forms are `True` for the corresponding image.

NLVR has four splits for training, development, public testing, and hidden testing. We follow the original splits for the training and development sets. Following the recent public release of the hidden testing set, we merge the public and hidden testing sets into a single public test split.

A.3 Annotations for Reward Computation

The NLVR annotations include the truth-value of each statement with regard to the images paired with it in the data. Once we manipulate an image (i.e., change the state in our interactive environment), the truth-value annotation does not hold. A key challenge for creating an interactive environment using the NLVR data is the need for an accurate evaluation of the natural language statement for *every* possible state (i.e., image), as required for reward computation (Section 2).

We address this challenge by annotating each statement $\bar{x}$ with an executable boolean Python program representing its meaning, $\mathcal{E}^{\bar{x}}$ in Section 2. The Python programs operate on the underlying structured representation. Each program returns `True` for every image that satisfies the constraints specified in the corresponding statement, and `False` otherwise. In general, there are many states that satisfy any given statement, many more than provided with the original NLVR images.

The programs are written using an API defined over the structured representations. We base the API design on the logical ontology designed for NLVR's structured representations by Goldman et al. [2018], which we extend to include a total of 66 functions. Figure 2 shows two examples of logical forms paired with their corresponding statements.

We use the freelancing platform Upwork[6] for annotation. We recruit three annotators based on preliminary screening of their fluency in English and competency in Python. We de-duplicate the naturally occurring sentences in the data, collect 2,666 annotations at a total cost of $3,756, and keep 2,661 valid annotations.

All the sentences in the dataset are randomly distributed to the annotators, each with an example image. Every sentence is annotated with a logical form by one annotator. Each logical form is evaluated against a corresponding hidden validation set, and must pass all the tests.

[6] `https://www.upwork.com`

B Related Work

There is significant and increasing interest in RL conditioned on natural language. Various strategies are deployed to resolve language semantics for reward computation, mostly by strict control of the language or through approximations.

Maybe the most common approach is to control the language by using synthetic language backed by a formal representation [Narasimhan et al., 2015, Johnson et al., 2017a,b, Côté et al., 2018, Chevalier-Boisvert et al., 2019, Co-Reyes et al., 2019, Jiang et al., 2020]. Although synthetic language allows studying the problem of learning high-level concepts, many of the complexities of natural language are stripped away, and such approaches run the risk of reducing the language learning challenge to reverse engineering the hand-crafted generation process.

An alternative that allows for natural language while retaining the control of its semantics is to generate the target sequence of decisions (i.e., task demonstration), and solicit post-hoc instructional language [Shridhar et al., 2020, 2021, Hanjie et al., 2021]. While this process uses human-written language, it potentially implicitly retains the regularities of the demonstration generation procedure.

Others have carefully designed the underlying environment to simplify termination state evaluation given demonstrations, for example, with a sparse graph-based structure [Anderson et al., 2018, Chen et al., 2019, Ku et al., 2020]. However, recent work shows the potential for evaluation fidelity issues even in these settings [Jain et al., 2019].

In contrast to previous approaches, we emphasize using human-written natural language and avoid constraining the task to simplify reward evaluation. We also opt to not use underlying hand-crafted procedures as stimuli for the writing. *lil*Gym prioritizes exact reward computation rather than automated approximations to allow for relatively clean benchmarking of learning methods.

Our annotation of natural language statements with programs is inspired by the annotation of data for supervised learning of semantic parsers [Zelle and Mooney, 1996, Zettlemoyer and Collins, 2005, Suhr et al., 2018]. The Python API of our environments is based on the semantic parsing work of Goldman et al. [2018]. Robust semantic parsers can assist in automating our annotation process.